AN EXPERIMENTAL AND KINETIC MODELLING STUDY OF PYROLYSIS AND COMBUSTION OF ACETONE-BUTANOL-ETHANOL (ABE) MIXTURES

Kevin M. Van Geem*, Alberto Cuoci, Alessio Frassoldati**, Steven P. Pyl*, Guy B. Marin*, Eliseo Ranzi****
eliseo.ranzi@polimi.it
* Laboratory for Chemical Technology, Universiteit Gent, Krijgslaan 281, S5, 9000 Gent, Belgium
** Dipartimento di Chimica, Materiali e Ingegneria Chimica – Politecnico di Milano –Piazza Leonardo da Vinci 32, 20131 Milano, Italy

Abstract
Bio-butantol is being studied extensively as alternative to conventional fuels due to its propensity of decreasing soot formation and improving the octane number of gasoline, resulting in renewed interest in the the acetone-butanol-ethanol (ABE) fermentation process and combustion of mixtures of acetone, butanol and ethanol. Therefore in this work a detailed mechanism for the pyrolysis and oxidation of ABE is presented containing ~200 species and ~6000 reactions. The mechanism is validated against newly acquired pyrolysis data. Laminar flame speeds computations of alcohols and ABE complement the detailed comparisons of the pyrolysis data and allow to further validate the combustion behaviour of bio-butanol.

Introduction
The study and use of oxygenated hydrocarbons, or biofuels, has become prevalent in the twenty-first century as the world searches for renewable energy sources. While ethanol has been the primary commercially-used fuel additive, recent research has been shifting towards the study of longer-chain alcohols because of their larger energy densities; lower miscibility in water, their greater compatibility when blended with conventional fuels or utilized in conventional engines; their lower vapor pressure; and their lower heat of vaporization. Pioneered by Chaim Weizmann in the UK at the time of World War I, the industrial acetone–butanol–ethanol (ABE) production using *solventogenic clostridia* was a very successful industrial fermentation during the early part of the twentieth century. The production of acetone–butanol by an isolated/pure microorganism was one of the first large-scale industrial microbial processes for chemical production, but lost all competitiveness with petrochemical synthesis in the 50's and 60's. The recent high oil prices have focused research attention again to this classical route for the production of butanol from biomass. Companies such as ButylFuel, Cathay Industrial, and others have provided new strains and process solutions for ABE fermentation, making the reintroduction of large-scale ABE fermentation increasingly feasible [1]. The key problems associated with the bioproduction of butanol are the cost of substrate and butanol toxicity/inhibition of the fermenting microorganisms, resulting in a low butanol titer in the fermentation broth. Advances in integrated fermentation and in situ product removal processes have resulted in a dramatic reduction of process streams, reduced butanol toxicity to the fermenting microorganisms, improved substrate utilization, and overall improved bioreactor performance. [2]

Despite this renewed interest in the ABE production the thermochemical conversion, i.e. combustion, oxidation and pyrolysis of ABE mixtures has remained largely unstudied. Therefore a fundamental mechanism is developed for combustion and pyrolysis of ABE

mixtures. This mechanism has been validated with new pyrolysis data and published laminar flame speeds obtained from Veloo and Egolfopoulos [3] and Veloo et al. [4].

Experimental

Experiments studying the pyrolysis of the ABE mixture were conducted in the bench-scale set-up of the Laboratory for Chemical Technology (LCT) of Ghent University [5]. A schematic of the experimental apparatus is shown in Figure 1. The unit can be divided into the feed, reaction, and analysis sections. First the ABE mixture is pumped into a vaporizer; the vaporizer is filled with quartz pellets to allow for a smooth evaporation. If desired, steam can be added as a diluent. The superheated vapor leaving the vaporizer at 523 K is further heated before entering the reactor section.

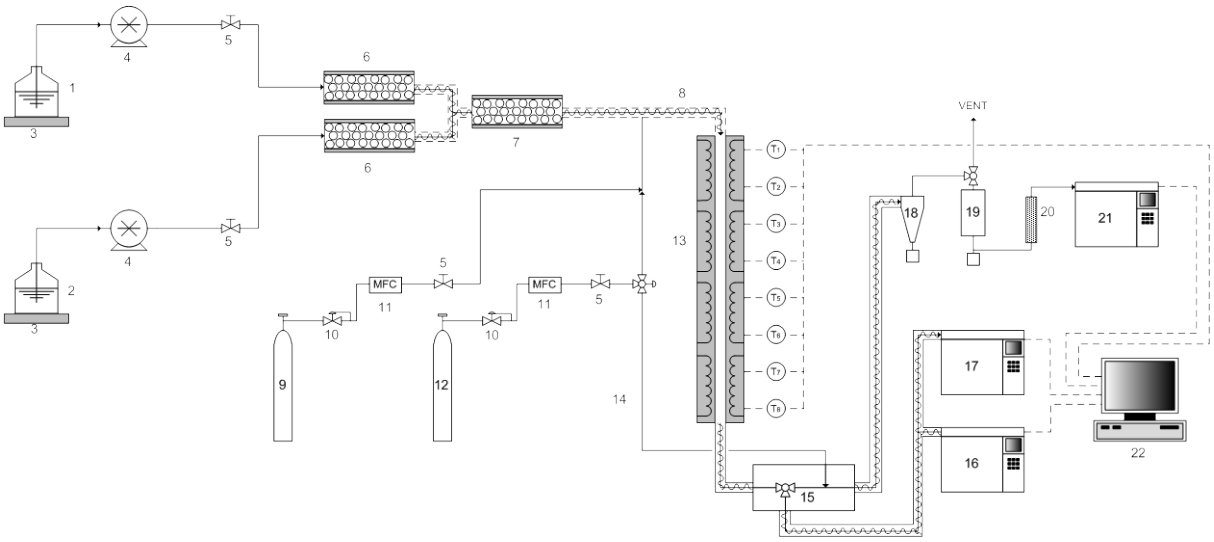

Figure 1. Schematic of the experimental pyrolysis set-up.

1: ABE vessel, 2: water vessel, 3: electronic balance, 4: pump, 5: valve, 6: evaporator, 7: mixer, 8: heater, 9: air, 10: pressure regulator, 11: mass flow controller, 12: nitrogen, 13: reactor, 14: nitrogen internal standard, 15: oven, 16: GC for formaldehyde and water, 17: GC×GC for C_5^+, 18: cyclone, 19: condenser, 20: dehydrator, 21: GC for C_4^-, 22: data acquisition

The reactor is a 1.475-m long, 6-mm internal diameter tube, made of Incoloy 800HT (Ni, 30-35; Cr, 19-23; and Fe, >39.5 wt %). There are eight thermocouples along the reactor, measuring the process gas temperature. The reactor is heated electrically and placed vertically in a rectangular furnace. The furnace is divided into four separate sections which can be heated independently to set a specific temperature profile. To compensate for heat losses near the outlet of the reactor, an extra heater is placed at the bottom of the furnace, so that the temperature will only drop at the outlet of the reactor. The pressure in the reactor is controlled by a back pressure regulator downstream from the outlet of the reactor. Two manometers are situated at the inlet and outlet of the reactor to measure the coil inlet pressure (CIP) and the coil outlet pressure (COP). The pressure drop over the reactor is negligible. Pyrolysis is observed to occur in the reactor when T > 823 K.

First the reactor is heated to the desired temperature profile and once the desired profile is attained, the feedstock is pumped into the evaporator; no water is fed in these experiments. The feedstocks were high purity n-butanol, acetone and ethanol (99.5% > pure), obtained from Acros Organics (Belgium). The evaporated feedstock flows through the reactor; the flow rate of the feedstock is controlled by a pulse free micro pump and calibrated by an electronic

balance. A fixed amount of N_2 is continuously added to the reactor effluent. This N_2 stream acts as an internal standard and allows the absolute yields of the individual effluent components to be determined.

Before cooling the effluent, a sample is taken online for analysis and injected on both the GC for formaldehyde and water analysis and the GC for the C_5^+ analysis. In the sample box the temperature is maintained above 523 K. This allows measuring polyaromatic components up to pyrene and chrysene in a single run [6]. The heaviest components observed in the reactor effluent are naphthalene and traces of methylnaphthalene and biphenyl. Next the reactor effluent is quenched and the liquid and tar are separated from the cooler exit by means of a knock-out vessel and cyclone. From the remaining gas a fraction is withdrawn for analysis on the refinery gas analyzer GC while the remainder of the effluent stream is directed to the vent.

Decoking of the reactor coil is performed by raising the reactor temperature to 1163 K and feeding pressurized air. The amount of coke formed during pyrolysis was marginal; under the most severe conditions, less than 1-gram of coke (i.e. <0.09% of ABE) is deposited on the reactor wall during 6-hours of cracking.

The conversion of the ABE mixture is varied by changing the temperature profile along the tubular reactor. An overview of the experimental conditions is given in Table 1. For each set of process conditions, at least two duplicate tests were performed to verify the results' reproducibility. Several different temperature profiles were studied, with coil outlet temperature (COT) ranging from 873 K to 1073 K. These set of conditions correspond to a range of n-butanol conversions from 30% to nearly complete conversion (> 98%).

	Range
T_{inl} [K]	673
T_{avg} [K]	880 – 1010
COP_{PR} [10^5 Pa]	1.5-1.7
Hydrocarbon Flow rate [g s^{-1}]	6.66 10^{-2}
Conversion [%]	32 – 98
Residence time [s]	0.85 – 1.2

Table 1. Overview of experimental conditions for the pyrolysis of ABE in the bench scale set-up

The analysis section of the pyrolysis setup is similar to the one discussed previously. The effluent sample taken online at lower temperature, i.e. the so-called C_{4-} sample, is analyzed on a Thermo Scientific Refinery Gas Analyzer (RGA), i.e. instrument 21 in Figure 1. Hydrogen, nitrogen, carbon monoxide, carbon dioxide, formaldehyde, and hydrocarbons up to C_2 are detected by a thermal conductivity detector (TCD). The C_1 to C_4 hydrocarbons are also analyzed with the RGA using a flame ionization detector (FID). This analysis takes approximately 20 minutes. The effluent sample taken at high temperature, before condensation of any of the effluent components, is automatically injected into and analyzed by both the formaldehyde GC and a Detailed Hydrocarbon Analyzer (DHA), i.e. instruments 16 and 17 in Figure 1. The implementation of an additional GC for formaldehyde and water, before cooling the effluent, is necessary because of the limited response on a FID and difficulties in separating them chromatographically from light C2 and C3 hydrocarbons. This GC is equipped with a TCD and the analyzed sample is taken on-line and at high temperature (approximately 523 K), i.e. before condensation of water and heavier product stream components. The separation is performed on 2 columns, first on a Rt-U-BOND capillary column (Restek, 1m x 0.32mm x 10μm) followed by a Rt-Q-BOND capillary column (Restek, 1m x 0.32mm x 10μm). In a single experiment the DHA was replaced by a GC×GC equipped

with a Time-of-Flight Mass Spectrometer (TOF-MS) to allow identification of every component in the effluent when cracking each of the ABE mixture. More than one hundred different components are observed and identified in the GC×GC TOF-MS chromatogram. Figure 2 shows part of the GC×GC chromatogram during one of the ABE experiments. The settings and the characteristics of the GC×GC can be found elsewhere [6]. The increased separation power of GC×GC makes it very suitable for analyzing complex effluents containing oxygenates.[Pyl et al., 2011] The 1st dimension separation is based on volatility, the 2nd on polarity. Major products formed during the cracking of ABE include CO, methane, ethene, propene, acetaldehyde, 1-butene, (E)- and (Z)-2-butene and unreacted acetone, butanol and ethanol. Minor products, such as formaldehyde, methanol, butanal, ketene, and 1,3-butadiene are also found in the effluent. Small amounts of benzene, toluene, xylenes, and ethylbenzene, and even traces of naphthalene and biphenyl, are detected. Peak identification and integration of the FID chromatogram is performed by a commercial integration package, GC-Image (Zoex Corp.), using the information obtained from GC×GC TOF-MS analysis.

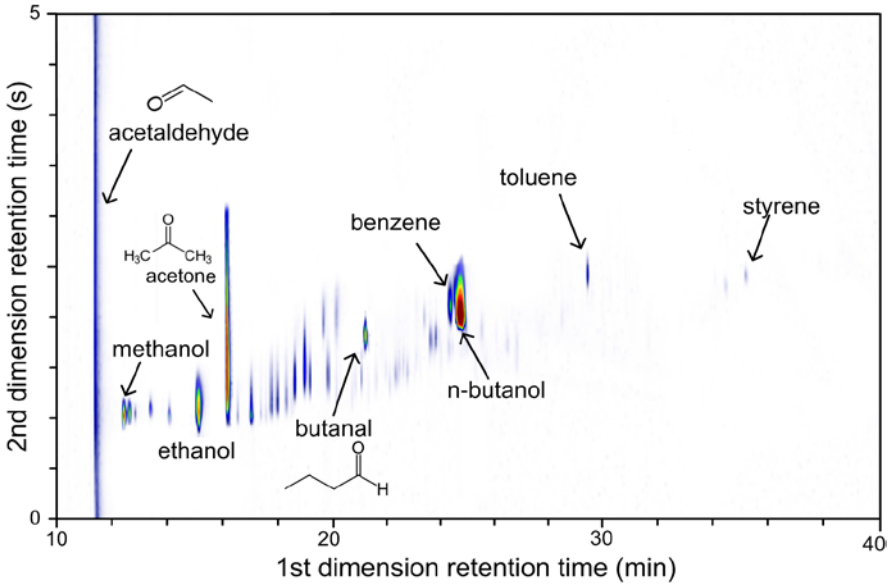

Figure 2. On-line GC×GC TOF-MS chromatogram obtained for ABE cracking

Calculations are based on the absolute flow rates of the effluent components. The flow rates of hydrogen, methane, carbon monoxide, and C_2 hydrocarbons are calculated using the peak areas of the RGA-TCD, the experimentally determined relative response factors for this instrument, and the known amount of nitrogen added to the reactor effluent. The mass flow rates of the other components are then calculated using the reference component system [5]. The relative response factors f_i for all major components, including all oxygenates, were determined experimentally, while the response factors for the minor hydrocarbons were calculated using Equation (1).

$$f_i = \frac{M_i}{N_{C,i}} \cdot \frac{1}{M_{CH_4}} \tag{1}$$

M_i is the molecular mass of component i with $N_{C,i}$ carbon atoms. The flow rates of the other components are then calculated using the methane flow rate as the normalization factor. The product yields are calculated according to Equation (2). y_i is the yield of compound i, F_i is the mass flow rate of compound i in the effluent stream, and F_0 is the mass flow rate of the hydrocarbon feed.

$$y_i = \frac{F_i}{F_0} \times 100 \qquad (2)$$

Small fluctuations (8.0277×10^{-3} g s^{-1} N_2 ± 2.78×10^{-5} g s^{-1}) in the nitrogen internal standard can result in incomplete balances. In the present study elemental balances for carbon, oxygen, and hydrogen closed within 0.5%. However, because all components can be identified the results were scaled to 100%.

Kinetic model and mathematical methods

The detailed oxidation mechanism is adopted from a more complete kinetic model developed for the pyrolysis and combustion of hydrocarbon fuels with up to 16 carbon atoms [7,8] consisting of over 10,000 reactions and 350 species. Thermochemical data for most species are obtained from the CHEMKIN thermodynamic database [9]. For those species whose thermodynamic data are unavailable, a group additive method (Benson) was used to estimate these properties. The complete mechanism, including thermodynamic and transport properties, is available in CHEMKIN format [http://creckmodeling.chem.polimi.it].

The overall kinetic scheme was developed based on hierarchical modularity and a reduced sub-mechanism, simply containing the high temperature mechanism, acetone and alcohol fuels is here adopted. This kinetic scheme contains ~200 species and ~6000 reactions. Pyrolysis and oxidation of ethanol, propanol and butanol isomers has been the subject of very recent kinetic works [10, 11, 8]. Figure 3 shows a schematic picture of the n-butanol decomposition and oxidation mechanism.

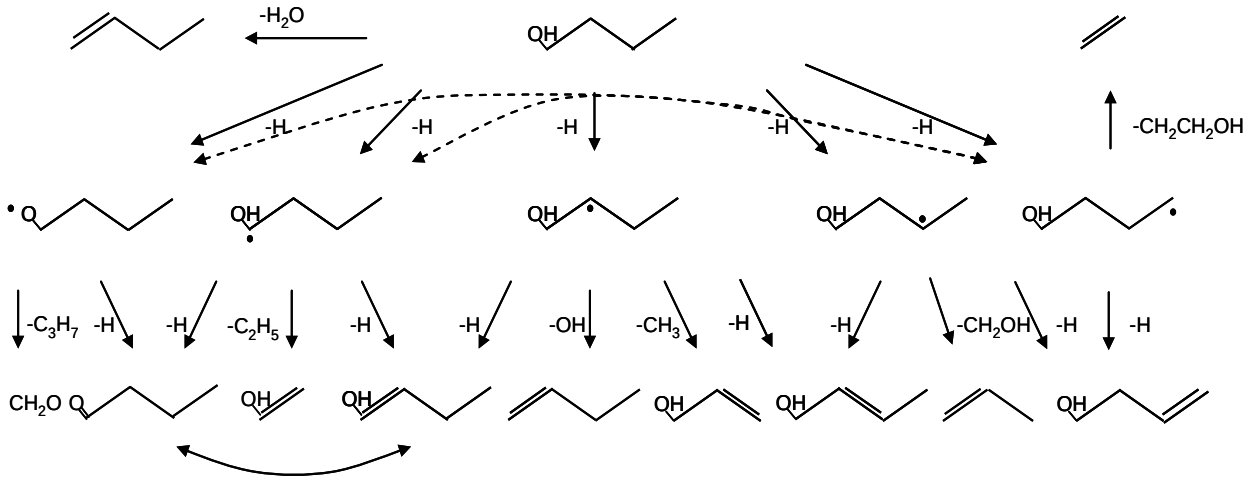

Figure 3. n-Butanol decomposition mechanism.

The dominant reaction path for the decomposition of acetone has been extensively studied [12, 13, 14]:

$CH_3COCH_3 \rightarrow CH_3COCH_2 \rightarrow CH_2CO \rightarrow CH_2O \rightarrow CO \rightarrow CO_2$.

Saxena et al. [15] observed that the measured dissociation rate $CH_3COCH_3 \rightarrow CH_3CO + CH_3$ is in close accord with the one already proposed by Sato and Hidaka [12]. However, the decomposition could be complicated by the molecular paths $CH_3COCH_3 \rightarrow CH_4 + CH_2CO$ or even $CH_3COCH_3 \rightarrow CO + CH_3CH_3$. These might occur through '*roaming methyl*': it is

perfectly possible for the ultimate products to be essentially the same from either radical or molecular paths.
Table 2 reports the main primary reactions of acetone decomposition.

			A	n	E
CH_3COCH_3	→	CH_3CO+CH_3	7.11×10^{21}	-1.57	354500
CH_3COCH_3+H	→	$CH_3COCH_2 + H_2$	6.00×10^{10}	0	42000
$CH_3COCH_3 + O$	→	CH_3COCH_2+OH	5.41×10^{03}	2	21000
CH_3COCH_3+OH	→	$CH_3COCH_2 + H_2O$	1.60×10^{03}	2	-1000
$CH_3COCH_3 + CH_3$	→	$CH_3COCH_2+CH_4$	1.56×10^{02}	2	32000
CH_3COCH_2	→	$CH_2CO + CH_3$	1.00×10^{11}	0	130000
CH_3CO+M	→	CH_3+CO+M	2.50×10^{12}	0	60300
CH_3COCH_3+H	→	$CH_3CHO+CH_3$	2.00×10^{10}	0	21000

Table 2. Main primary reactions of acetone decomposition (Units are mole, l, s, J).

The pyrolysis reactor was modeled using a Plug Flow Reactor solver of DSMOKE software package [10,17]. In fact, as the computed temperature and concentration profiles exhibited only small radial gradients throughout the length of the reactor, modeling the reactor as plug flow is valid, as discussed in a previous study on n-butanol [5].

Laminar flame speeds were calculated for the steady, freely propagating, adiabatic flames in the doubly infinite domain, without radiative heat transfer while allowing for Soret diffusion. The conservation equations with proper boundary conditions [16] were discretized by means of conventional finite differencing techniques with non-uniform mesh spacing. Diffusive and convective terms use central and upwind differencing respectively [17].

Comparisons of pyrolysis experiments

Figure 4 reports the conversion of the three components. Panel a) of this figure shows that the predicted n-butanol conversion versus temperature properly matches the experimental measurements. The bottom figures report the decomposition of acetone and ethanol versus butanol conversion. The fair agreement between model predictions and experimental measurements confirms that acetone has a lower reactivity, when compared to ethanol and butanol.

Figures 5 to 7 report the yields of the major species from the pyrolysis of ABE mixture. Alkenes as well as major oxygenated species are properly predicted by the kinetic model. The same is also true for the minor heavier species reported in Figure 7.

Figure 6 shows a relevant deviation of butanal at ~30% butanol conversion. To better clarify this point, Figure 8 shows the flux and sensitivity analysis for butanal. H-abstraction reaction of the acyl H-atom of butanal is the most sensitive disappearance reaction, while the competition between the decomposition of RBU1OHα to form butanal or acetaldehyde and the decomposition of RBU1OHβ to form butanal or 1-butene are in the set of the most sensitive reactions. Both the analyses of Fig. 8 indicate that also the direct molecular dehydrogenation reaction of butanol further contributes to butanal formation. Based on this analysis the butanal deviation can be considered as an outlier, and this will be verified by carrying out additional experiments at even lower conversions.

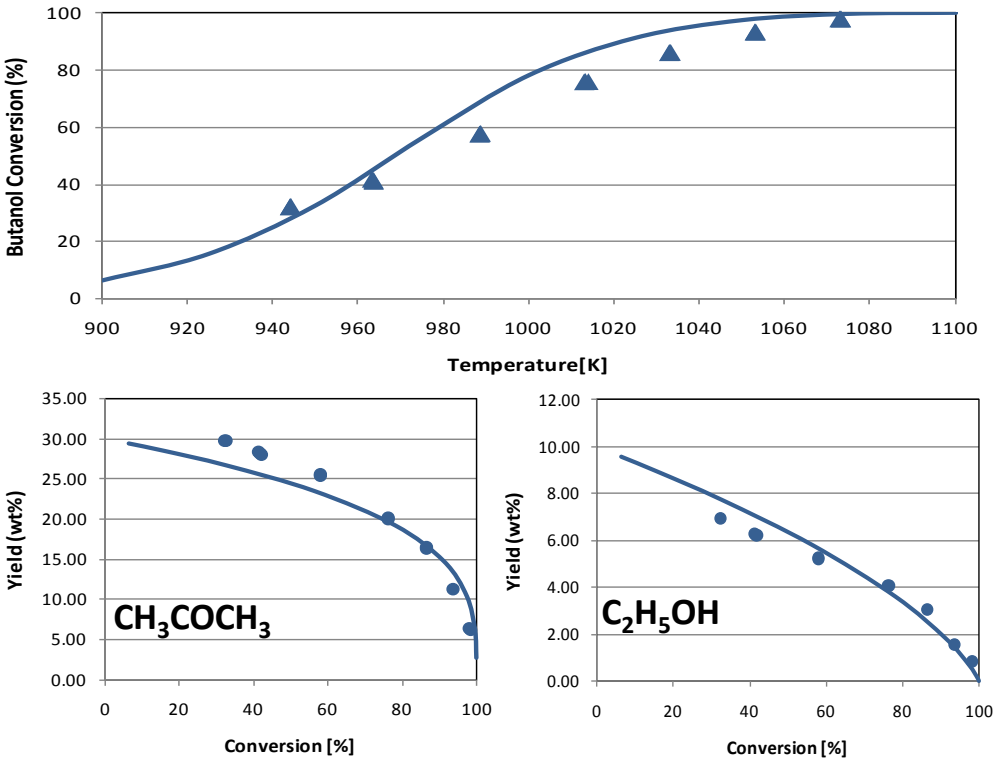

Figure 4. a) n-Butanol conversion versus temperature [K]. b) acetone and ethanol yields versus butanol conversion.

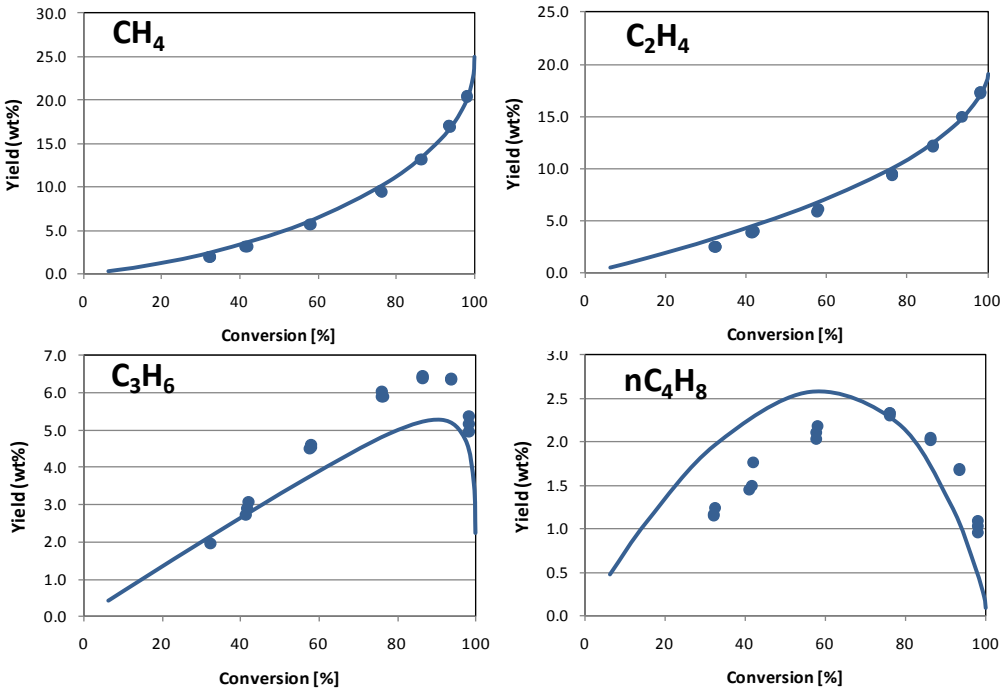

Figure 5. Methane, ethene, propene and butene yields versus butanol conversion.

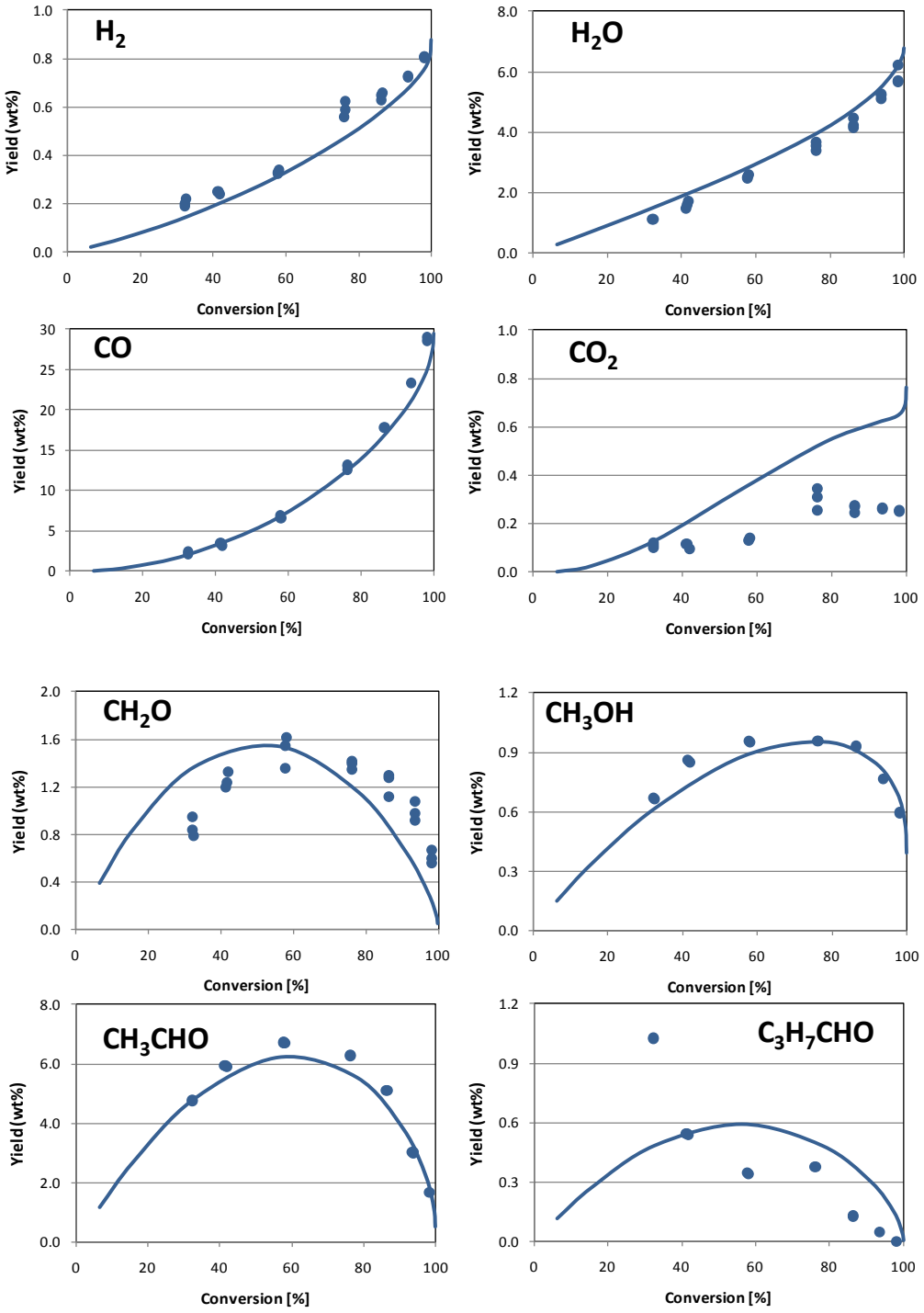

Figure 6. Yields of Hydrogen, and major oxygenated species versus butanol conversion.

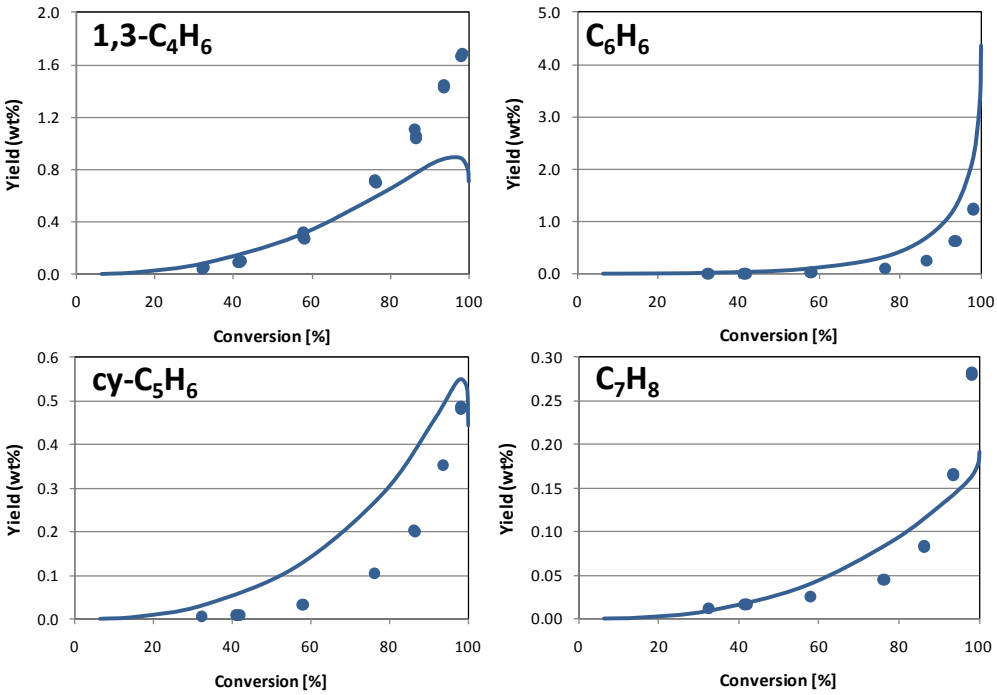

Figure 7. Yields of minor heavier species versus butanol conversion.

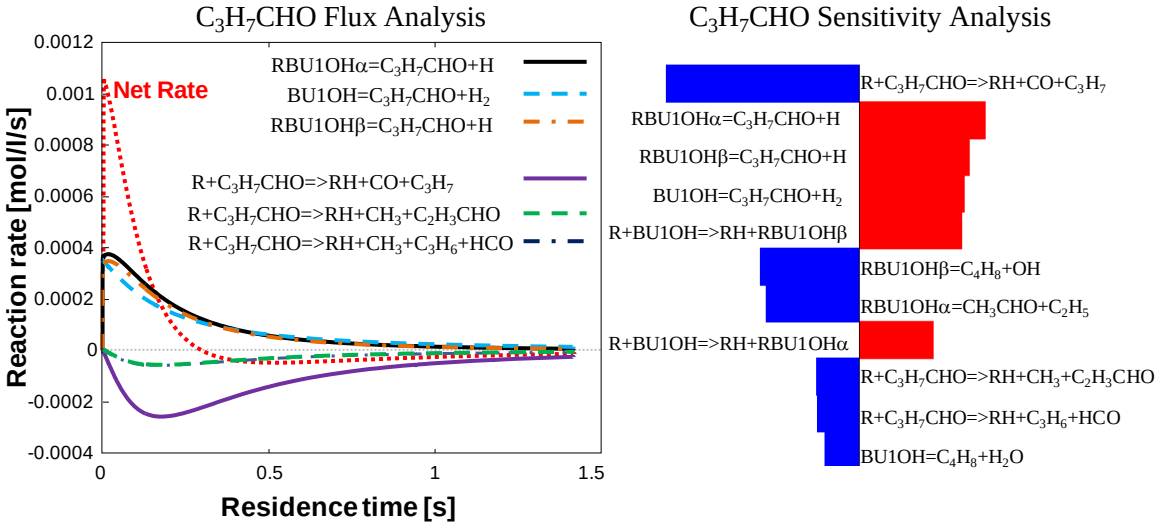

Figure 8. Flux and Sensitivity analysis for butanal at 1000 K and 1.7 atm.

Laminar flame speed of ABE mixture

Laminar speeds of premixed methanol, ethanol, and n-butanol flames at atmospheric pressure were recently determined [3,4]. These results show that the laminar flame speeds of methanol are higher as compared to those of ethanol and the heavier alcohol flames, under fuel-rich conditions. Furthermore, while the laminar flame speeds of methanol are consistently higher than those of methane, the flame speeds of ethanol, n-propanol and n-butanol are similar to those of the corresponding n-alkanes. The effect of hydroxyl substitution of hydrogen is to enhance the laminar flame speeds for methanol, as compared to methane, while having minor differences for ethanol as compared to ethane.

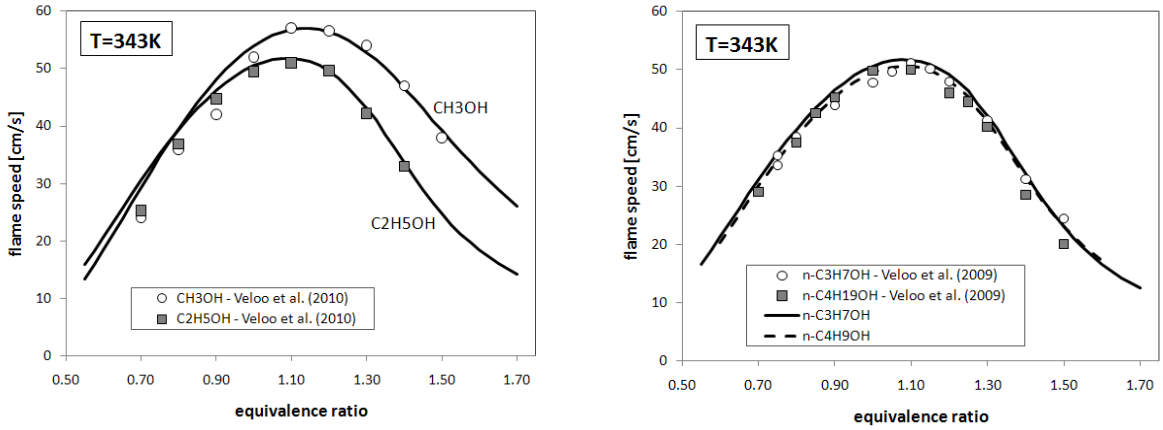

Figure 9. Laminar burning velocity of pure components at 343 K.: (a) flame velocity of methanol and ethanol [3]; (b) flame velocity of n-propanol and n-butanol [18,4]

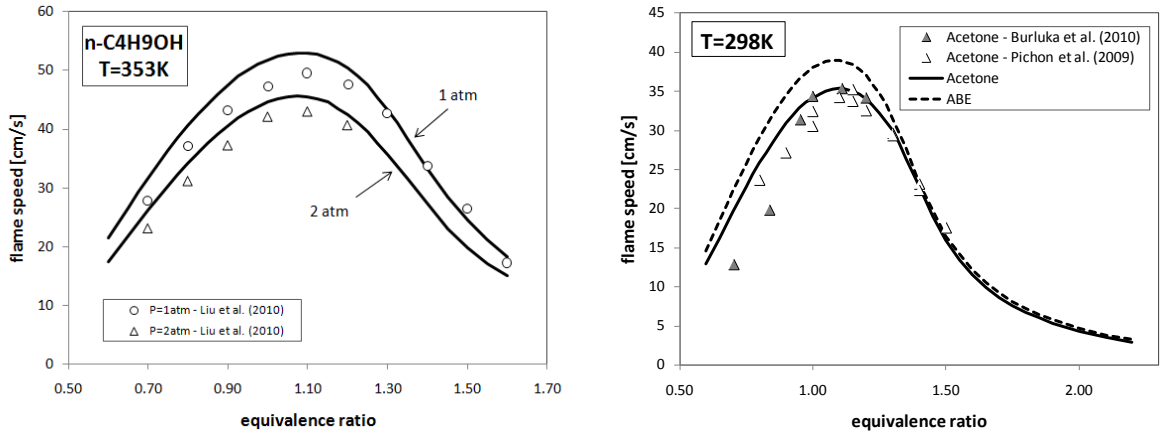

Figure 10. (a) Laminar burning velocity of n-butanol flames in air at 1 and 2 atm and 353 K [19]. (b) Laminar flame speeds of acetone [13,20] and ABE at 298 K.

Figure 9 shows the very satisfactory agreement between experimental measurements and model predictions for the pure alcohols, from methanol to n-butanol. As already observed by Veloo et al. (2010), the laminar flame speed of methanol is the highest, while marginal differences are experimentally and numerically observed amongst ethanol, n-propanol and n-butanol. The difference in the laminar flame speeds of methanol with those of the heavier alcohols is mainly due to the kinetics rather than to the different adiabatic flame temperatures. H abstraction reactions on methanol mainly form CH_2O without significant CH_3 radical formation. Higher concentrations of CH_3 and CH_4 are observed in ethanol and butanol flames and they are mainly due to the production of CH_3CHO and the subsequent decomposition of the CH_3CO radicals. The uniqueness of the methanol reaction mechanism is the limited CH_3 formation with a prevailing H radical path with branching reactions. Figure 10a shows the comparison of model predictions and the experimental measurements of Liu et al. [19] for n-butanol at 1 and 2 atm. The flame speeds at 298 K and 1 atm of pure acetone in air were measured in a spherical bomb and a maximum flame speed of ~35 cm s^{-1} at Φ = 1.15 was indicated by Pichon et al. [13]. Figure 10b compares model predictions with these measurements and also compares the predicted laminar flame speed of ABE with the corresponding one of acetone. As expected, the ABE laminar flame speed is higher than the acetone one and lower than ethanol and butanol burning rates. Thus the octane rating of ABE mixture is higher when compared with the one of pure n-butanol fuel.

Conclusions

A detailed mechanism for the pyrolysis and combustion of mixtures of acetone n-butanol and ethanol has been constructed. The model has been validated against multiple types of experiments – flames, and pyrolysis experiments – and varying reaction conditions. For the pyrolysis experiments the model is able to capture all the trends of the major and minor products correctly apart from butanal. Additional experimental verification is necessary to clarify these discrepancies at low conversions for this product. The calculated ABE laminar flame speed is higher than the one of acetone and lower than the laminar flame speed of ethanol and butanol, which agrees with the observed experimental flame speeds. Hence, this mechanism should be a useful seed mechanism for future modelling of blends of fuels blends containing oxygenates and hydrocarbons.

Acknowledgements

The work at Politecnico di Milano was supported by the Italian Government MSE/CNR (Biofuel Project). The Authors also acknowledge useful discussions with Prof. Tiziano Faravelli in the behalf of European COST Action CM 0901 'Detailed chemical kinetic models for cleaner combustion'.
KVG held a Postdoctoral Fellowship of the Fund for Scientific Research, Flanders, Belgium. SPP and GBM acknowledge the financial support from the Long Term Structural Methusalem Funding by the Flemish Government.

References

[1] Ezeji T. C., Qureshi N., Blaschek H. P., "Acetone butanol ethanol (ABE) production from concentrated substrate: reduction in substrate inhibition by fed-batch technique and product inhibition by gas stripping", *Appl Microbiol Biotechnol* 63:653–658, (2004).
[2] Ezeji T. C., Qureshi N., Blaschek H. P., "Bioproduction of butanol from biomass: from genes to Bioreactors", *Current Opinion in Biotechnology*, 18:220–227 (2007).
[3] Veloo P. S. and F. N. Egolfopoulos, "Flame Propagation of Butanol Isomers/Air Mixtures", *Proceedings of the Combustion Institute* 33 (1):987-993, (2011).
[4] Veloo P. S., Wang Y. L., Egolfopoulos F. N., Westbrook C. K., "A comparative experimental and computational study of methanol, ethanol, and n-butanol flames", *Combustion and Flame* 157(10): 1989-200 (2010).
[5] Harper, M.R., Van Geem K. M., Pyl S. P., Marin G. B., Green W. H., "Comprehensive reaction mechanism for n-butanol pyrolysis and combustion", *Combustion and Flame* 158:16–41 (2011).
[6] Van Geem, K. M., Pyl S.P., Reyniers M.F., Vercammen J., Beens J., Marin G. B., "Online analysis of complex hydrocarbon mixtures using comprehensive 2D gas chromatography", *Journal of Chromatography A*, 1217:6623–6633 (2010).
[7] Ranzi E., "A wide-range kinetic modeling study of oxidation and combustion of transportation fuels and surrogate mixtures", *Energy and Fuels* 20 (3):1024-1032 (2006).
[8] Grana R., Frassoldati A., Faravelli T., Niemann U., Ranzi E., Seiser R., Cattolica R., Seshadri K., An experimental and kinetic modeling study of combustion of isomers of butanol, *Combustion and Flame* 157(11): 2137-2154 (2010).
[9] Kee, R. J., Rupley F., Miller J. A., Chemkin II: A Fortran Chemical Kinetics Package for the Analysis of Gas-Phase Chemical Kinetics. Sandia Report, Sandia National Laboratories (1989).
[10] Frassoldati A., Cuoci A., Faravelli T., Niemann U., Ranzi E., Seiser R., Seshadri K., "An experimental and kinetic modeling study of n-propanol and iso-propanol combustion", *Combustion and Flame* 157(1): 2-16 (2010).

[11] Frassoldati A., Cuoci A., Faravelli T., Ranzi E., Kinetic Modeling of the Oxidation of Ethanol and Gasoline Surrogate Mixtures, *Combustion Science and Technology* 182(4-6): 653-667 (2010).
[12] Sato K., Hidaka Y., "Shock-tube and modeling study of acetone pyrolysis and oxidation", *Combustion and Flame* 122 (3):291-311 (2000).
[13] Pichon, S., Black G., Chaumeix N., Yahyaoui M., Simmie J.M., Curran H.J., Donohue R., "The combustion chemistry of a fuel tracer: Measured flame speeds and ignition delays and a detailed chemical kinetic model for the oxidation of acetone", *Combustion and Flame* 156:494–504 (2009).
[14] Chong C. T., Hochgreb S., "Measurements of laminar flame speeds of acetone/methane/air mixtures", *Combustion and Flame* 158:490–500 (2011).
[15] Saxena, S., Kiefer J. H., Klippenstein S. J., "A shock-tube and theory study of the dissociation of acetone and subsequent recombination of methyl radicals", *Proceedings of the Combustion Institute* 32:123–130 (2009).
[16] Smooke M. D., Rabitz H., Reuven Y., Dryer F. L., "Application of sensitivity analysis to premixed hydrogen-air flames", *Combustion Science and Technology* 59:295-319 (1983).
[17] Frassoldati A., Grana R., Cuoci A., Faravelli T., Ranzi E., Kelley A.P., Law C.K., "Hierarchical and Comparative Kinetic Modeling of Laminar Flame Speeds of Reference Fuels and Their Mixtures", submitted to *Progress in Energy and Combustion Science* (2011).
[18] Veloo P. S., Egolfopoulos F.N., Westbrook C. K.,"Studies of n-Propanol/Air and iso-Propanol/Air Premixed Flames", Fall Meeting of WSS/CI - Paper # 09F-44 (2009).
[19] Liu W., Kelley A.P., Law C.K., "Non-premixed Ignition, Laminar Flame Propagation and Mechanism Reduction of n-Butanol, iso-Butanol and Methyl Butanoate", *Proceedings of the Combustion Institute* 33(1): 995-1002 (2011).
[20] Burluka, A.A., Harker M., Osman H., Sheppard C.G.W., Konnov A.A., "Laminar burning velocities of three C_3H_6O isomers at atmospheric pressure", *Fuel* 89(10): 2864-2872 (2010).